

**THE DEVELOPMENT OF GELATIN BASED TISSUE ADHESIVES  
FOR USE IN SOFT TISSUE BIOMEDICAL APPLICATIONS**

by

Kristen L. Droesch

Thesis submitted to the Faculty of Virginia Polytechnic Institute and State  
University in partial fulfillment of the requirements for the degree of

MASTER OF SCIENCE

IN

MATERIALS SCIENCE AND ENGINEERING

Brian J. Love Ph.D., Chair

Jonette Rogers Foy Ph.D.

Sean G. Corcoran Ph.D.

Keywords: Gelatin, Resorcinol, Glyoxal, Tissue Adhesive

July 28, 1999

Blacksburg, VA

Copyright 1999, Kristen L. Droesch

# THE DEVELOPMENT OF GELATIN BASED TISSUE ADHESIVES FOR USE IN SOFT TISSUE BIOMEDICAL APPLICATIONS

by

Kristen L. Droesch

Dr. Brian J. Love, Chairman

Department of Materials Science and Engineering

## (ABSTRACT)

Experiments were performed to characterize the pH, gelation time, diffusion processes, material properties, adhesive properties, and the drying variables on the material and adhesive properties of Gelatin Resorcinol Dialdehyde (GR-DIAL) tissue adhesives by varying formulation. Three adhesive formulations with altered weight content of water and glyoxal (a dialdehyde) were utilized. The adhesive formulations were characterized by pH and gelation time *in situ*, and absorption/desorption of water in the formed resin. Thermal analysis, mechanical testing, and lap shear adhesive bond testing were utilized to characterize fresh GR-DIAL adhesive formulations and formulations dried at 37°C. From the results, the diffusion processes, material and adhesive properties of the adhesive formulations were primarily affected by hydrogen bonding, chemical cross-linking, and the existence of bound water within the bulk adhesive. Formulations with increased glyoxal content had both a higher degree of cross-linking and proportion of bound water within the bulk adhesive. The increased number of chemical cross-links greatly increased the swelling resistance of the adhesives, while, the existence of bound water within the adhesive increased the resistance to drying, and plasticized the resin by depressing the resin glass transition temperature, and increased the adhesive ductility. Hydrogen bonding increased with increased gelatin content or decreased water content, resulting in increased strength and modulus of the adhesives as well as increased adhesive strength.

## ACKNOWLEDGEMENTS

The author would like to thank Dr. Brian Love for serving as advisor and chairman for my thesis committee in addition to his technical advice, moral, and financial support. I would like to thank Dr. Foy and Dr. Corcoran for agreeing to serve on my thesis committee. I also would like to thank Dr. Hugo Veit for providing me with the cowhide used for the experiments. I would like to thank the Center for Adhesive and Sealant Science for partial financial support of my project.

I would like to thank the following people that work in our lab group for their moral and technical support: Steve Clay, Patricia Dolez, Julie Dvorkin, Michelle Jensen, Mitch Jackson, Jennifer McPeak, Scott Steward, and Sumitra Subrahmanyam.

I would like to thank my family for their unconditional love and tremendous moral support throughout my life. I owe much gratitude to my mother Karen Droesch, my Aunt Barbara O'Hagan, and my grandmother Katherine Coffey who convinced and encouraged me to continue pursuing my Master's degree.

I would like to thank my friends Matt Mullen, Cori Evans and Heather Dunnigan for their moral support this past year and for dealing with me on a daily basis.

## TABLE OF CONTENTS

<b>Abstract .....</b>	<b>ii</b>
<b>Acknowledgements.....</b>	<b>iv</b>
<b>List of Tables .....</b>	<b>vi</b>
<b>List of Figures.....</b>	<b>vii</b>
<b>1. Introduction.....</b>	<b>1</b>
<b>2. Background and Literature Review .....</b>	<b>3</b>
2.1 Soft Tissue Structure and Composition .....	3
2.1.1 Collagen.....	6
2.1.2 Elastin .....	6
2.1.3 Mechanical Properties of Connective Tissue .....	7
2.2 The Use of Tissue Adhesives for Wound Closure .....	9
2.2.1 Gelatin Based Tissue Adhesives.....	10
2.3 Components of Hybridized Tissue Adhesives .....	12
2.3.1 Gelatin .....	12
2.3.2 Resorcinol.....	14
2.3.4 Cross-linking of Hybridized Tissue Adhesives with Aldehydes.....	15
2.3.4 Mechanisms of Degradation .....	17
2.4 Measurement of pH and Gelation Time of Tissue Adhesives.....	18
2.5 Drying and Swelling of Tissue Adhesives .....	19
2.6 Thermal Analysis.....	24
2.7 Tensile Testing .....	24
2.8 Stress Relaxation.....	25
2.9 Adhesion .....	28
2.9.1 Theories of Adhesion.....	28
2.9.2 Wetting and Contact Angle Measurements.....	29
2.9.3 Determination of Surface Tension From Contact Angle Measurements.....	31
2.9.4 Measuring Adhesive Bond Strength of Tissue Adhesives.....	32
2.9.5 Bond Strength Using Lap Shear Test .....	35
2.9.6 Adhesive Failure .....	36
<b>3. Experimental Procedures .....</b>	<b>37</b>
3.1 Materials and Fabrication .....	37
3.1.1 Materials .....	37
3.1.2 Formulation Variations .....	37
3.1.3 Fabrication Methods.....	38
3.2 Observations During Fabrication .....	41
3.2.1 pH Measurements.....	41
3.2.2 Gelation Time .....	41
3.3 Absorption/Desorption .....	42
3.3.1 Swelling Measurements.....	42
3.3.2 Drying Measurements.....	42
3.4 Thermal Analysis .....	43
3.4.1 Dynamic Mechanical Spectroscopy.....	43

3.4.2 Differential Scanning Calorimetry.....	44
3.4.3 Thermogravimetric Analysis.....	45
3.5 Mechanical Testing of Adhesives .....	46
3.5.1 Tensile Testing.....	46
3.5.2 Stress Relaxation.....	47
3.6 Adhesive Testing .....	48
3.6.1 Lap Shear Testing of Adhesive Bonded Glass Substrates.....	48
3.6.2 Lap Shear Testing of Adhesive Bonded Bovine Tissue .....	50
3.7 Optical microscopy .....	51
3.8 Statistical Analysis.....	51
<b>4. Results and Discussion.....</b>	<b>52</b>
4.1 Observations During Fabrication .....	52
4.1.1 pH and Gelation Time Measurements .....	52
4.2 Absorption/Desorption .....	55
4.2.1 Swelling Measurements.....	55
4.2.2 Drying Measurements.....	58
4.3 Thermal Analysis.....	62
4.3.1 Dynamic Mechanical Spectroscopy.....	62
4.3.2 Differential Scanning Calorimetry.....	66
4.3.3 Thermogravimetric Analysis.....	69
4.4 Optical Microscopy.....	74
4.5 Mechanical Testing of Adhesives .....	75
4.5.1 Tensile Testing .....	75
4.5.2 Stress Relaxation.....	82
4.6 Adhesive Testing .....	85
4.6.1 Lap Shear Testing of Adhesive Bonded Glass Substrates.....	85
4.6.2 Failure of Adhesive Bonds.....	89
4.6.3 Lap Shear Testing of Adhesive Bonded Bovine Tissue .....	90
<b>5. Summary of Results and Conclusions .....</b>	<b>92</b>
<b>6. Future Work.....</b>	<b>94</b>
<b>References.....</b>	<b>95</b>
<b>Appendix: Contact Angle Measurements of Glass Substrate .....</b>	<b>99</b>
<b>Vita .....</b>	<b>100</b>

## LIST OF TABLES

Table 2.1.1 Amino acid R groups.....	5
Table 2.2.1 Requirements of tissue adhesives .....	10
Table 2.9.1 Surface tension contributions for common liquids at 20 <sup>0</sup> C used in determining surface energy from contact angle measurements .....	32
Table 2.9.2 Summary of adhesive bond strengths found in the literature.....	34
Table 3.1.1 Weight fractions for three different GR-DIAL formulations.....	37
Table 4.1.1 Measurement of pH before and after gelation compared by formulation.....	53
Table 4.1.2 Gelation time (in seconds) compared by formulation .....	53
Table 4.2.1 Normalized percent mass uptake at swelling equilibrium by formulation.....	57
Table 4.2.2 Calculated diffusivity of adhesive formulations from swelling experiments...	57
Table 4.2.3 Equilibrium weight loss and percent residual water of dried adhesives .....	59
Table 4.2.4 Calculated diffusivity of adhesive formulations from drying experiments.....	61
Table 4.3.1 Average measured T <sub>g</sub> for fresh frozen and dried samples .....	63
Table 4.3.2 Average measured change in enthalpy of ice melt at heating rates of 3 <sup>0</sup> C/min and 10 <sup>0</sup> C/min (J/g) .....	67
Table 4.3.3 Weight loss as a function of temperature for aged and fresh frozen samples ..	73
Table 4.5.1 Average measured strength, elastic modulus, and strain at break by formulation .....	76
Table 4.5.2 Table of mechanical properties of skin .....	81
Table 4.5.3 Average relaxation fit parameters by formulation .....	83
Table 4.6.1 Table of average shear strength values for adhesive bonded glass substrates..	86
Table 4.6.2 Comparison of average shear strength of bovine skin to glass substrate adhesive specimens.....	90
Table 4.6.3 Table of measured adhesive strength of bonded tissue found in the literature with comparison to formulation C bonded to cow skin .....	91

## LIST OF FIGURES

Figure 2.1.1 Structural organization of connective tissue components .....	4
Figure 2.1.2 Condensation polymerization of amino acids forming polypeptide chain .....	4
Figure 2.1.3 Stress Strain curve for human thoracic aorta.....	7
Figure 2.1.4 Stress Strain curve for wet rat tail tendon .....	8
Figure 2.1.5 Stress Strain Curve for Wet Rat Back Skin.....	8
Figure 2.3.1 Characteristic shape of curve for viscosity ( $\eta$ ) versus time as gelatin solution is cooled .....	13
Figure 2.3.2 Structure of Resorcinol.....	14
Figure 2.3.3 Structure of aldehydes .....	15
Figure 2.3.4 Idealized representation of cross-linking of protein by glyoxal.....	16
Figure 2.3.5 Resin formed from condensation reaction of glyoxal and resorcinol.....	16
Figure 2.3.6 In vitro degradation rate of collagen as a function of molecular weight between cross-links .....	17
Figure 2.5.1 Sheet of thickness L used for diffusion equations .....	20
Figure 2.5.2 Example plot of equation 2.5.2 .....	20
Figure 2.6.1 Illustration of cross-linked chains in a network polymer .....	23
Figure 2.6.2 Illustration of possible existence of bound and unbound water in the bulk adhesive unbound water in the bulk adhesive .....	23
Figure 2.8.1 Illustration of stress relaxation resulting from constant applied strain .....	27
Figure 2.8.2 Maxwell model – spring and dashpot in series.....	27
Figure 2.8.3 Multiple Maxwell units in parallel used to simulate more complicated stress relaxation responses .....	27
Figure 2.9.1 Representation of a liquid wetting a solid surface and contact angle formed.	30
Figure 2.9.2 Butt joint test (a), lap shear joint test (b).....	33
Figure 2.9.3 Dimensions of lap joint used in stress concentration equations .....	36
Figure 2.9.4 Adhesive bond (a), cohesive failure of adhesive (b), cohesive failure of adherend (c), and interfacial failure (d).....	36
Figure 3.1.1 Fabrication procedure for experimental samples.....	39
Figure 3.1.2 Illustration of block samples fabricated for experiments .....	39
Figure 3.1.3 Illustration of dog bone test specimens.....	40
Figure 3.4.1 Illustration of three point bending mode.....	44
Figure 3.6.1 Illustration of lap shear test specimens .....	49
Figure 3.6.2 Illustration of dried lap shear test specimens.....	49
Figure 3.6.3 Illustration of lap shear sample with cow skin adherend .....	50
Figure 4.1.1 Graph of gelation time vs. pH measured before and after gelation.....	53
Figure 4.1.2 Graph of gelation time vs. gelatin weight % .....	54
Figure 4.2.1 Illustration of appearance of adhesives with swelling time .....	56
Figure 4.2.2 Typical graph of normalized mass vs. time for water absorption in adhesives .....	56
Figure 4.2.3 Graph of typical water absorption measurements fit to equation 2.5.2 .....	57

Figure 4.2.4 Typical graph of normalized mass vs. time for water desorption in adhesives .....	59
Figure 4.2.5 Graph of initial water and glyoxal content of adhesive formulations compared to weight loss of water due to drying.....	60
Figure 4.2.6 Graph of typical water desorption measurements fit to equation 2.5.2 .....	61
Figure 4.3.1 Typical DMS run for adhesive formulations.....	63
Figure 4.3.2 Dependence of glass transition temperature on glyoxal content for fresh frozen samples.....	64
Figure 4.3.3 Graph of glass transition temperature of dried adhesives as a function of residual water content.....	65
Figure 4.3.4 Typical DSC trace for adhesives .....	67
Figure 4.3.5 Change in enthalpy of the ice melt in adhesives as a function of glyoxal content.....	68
Figure 4.3.6 Representative weight loss thermogram for fresh frozen samples.....	70
Figure 4.3.7 First derivative of weight loss of fresh frozen samples.....	71
Figure 4.3.8 Representative weight loss thermogram for dried samples .....	72
Figure 4.3.9 First derivative of weight loss of dried samples .....	73
Figure 4.4.1 Optical micrograph of bulk adhesive showing bound and unbound water phases.....	74
Figure 4.5.1 Typical stress-strain curves for fresh frozen samples .....	77
Figure 4.5.2 Typical stress-strain curves for dried samples .....	78
Figure 4.5.3 Graph of strength and elastic modulus dependence on gelatin weight % for fresh frozen adhesives .....	79
Figure 4.5.4 Graph of strength and modulus of dried adhesives as a function of residual water content .....	80
Figure 4.5.5 Graph of strain at break as a function of residual water content of dried adhesives.....	81
Figure 4.5.6 Typical stress relaxation curve.....	83
Figure 4.5.7 Graph of relaxation behavior of the three formulations using average fit parameters .....	84
Figure 4.6.1 Typical average shear stress vs. distance curves for fresh lap shear samples	86
Figure 4.6.2 Typical average shear stress vs. distance curves for dried lap shear samples	87
Figure 4.6.3 Graph of the average shear strength of lap shear bonds as a function of gelatin content .....	88
Figure 4.6.4 Optical micrograph of glass slide adherend with traces of adhesive remaining on surface following testing.....	89
Figure A.1 Schematic Diagram of Rame' -Hart Goniometer.....	100
Figure A.2 Illustration of measurement of sessile drop using goniometer .....	100



## 1. INTRODUCTION

Wounds of soft tissue resulting from trauma or surgery require an adequate method for wound closure. Traditional methods of wound closure utilize sutures and staples, but the use of tissue adhesives as an alternative method for binding tissue has gained recognition in the last few decades. The use of tissue adhesives can lead to a rapid and satisfactory wound closure, and requires less surgical skill than traditional suturing.<sup>1</sup> The use of tissue adhesives can minimize the time spent in the operating room, reduce the time patients are under anesthesia, the loss of blood and need for transfusions, and other complications that may accompany wound closure,<sup>1</sup> thus minimizing cost and possible pain and suffering. Tissue adhesives for wound closure must meet several requirements: they must be biocompatible, not toxic, provide strong bonding, be tough and pliable, provide hemostasis, and be resorbable.<sup>1,2,3,4</sup>

Tissue adhesives have been fabricated from both natural and synthetic sources. Cyanoacrylate and polyurethane adhesives, fibrin glue, and several types of gelatin-based adhesives have been used experimentally and clinically for wound closure.<sup>1</sup> Hybrid gelatin-based adhesives consisting of gelatin and resorcinol cross-linked with formaldehyde, known as GRF, were first developed in the 1960's as an alternative to cyanoacrylate and polyurethane based adhesives which exhibited poor bonding strength in the presence of moisture.<sup>4,5</sup> In the last five to six years, due to toxicity concerns of formaldehyde usage, experimental work has been conducted on hybrid tissue adhesives cross-linked with a mixture of glutaraldehyde and glyoxal.<sup>5,6</sup>

Many motivations led to the development and experimental approach of gelatin resorcinol dialdehyde tissue adhesive investigated in this work. The preponderance of the available literature on hybrid tissue adhesives has been written from a clinical standpoint, and there was no evidence of an analysis from a materials perspective. The chemical formulations of hybrid tissue adhesives utilized in past work have not been explicitly given in the literature. Also, there has been no evidence in the literature of glyoxal being used as the sole cross-linking agent in GR-DIAL tissue adhesives. Formaldehyde and glutaraldehyde that have been used extensively in gelatin based tissue adhesives as the cross-linking agents are also used as fixatives and tanning agents and have specific toxicity concerns.<sup>1-2,4-8</sup>

The overall goal of this project was to understand the factors that control the material properties, the absorption/desorption of water and the variables introduced during the fabrication. Specifically, the objectives were to characterize pH and gelation time variation during the fabrication processes, the absorption/desorption of water as a function of formulation for GR-DIAL adhesives, and to characterize the thermal properties, mechanical properties and adhesive properties as a function of formulation and thermal aging. An additional objective was to measure the strength of adhesive bonded to bovine tissue and compare it to adhesive strength values found in the literature for similar test scenarios. Three formulations with altered weight fractions of water and glyoxal were utilized for testing. The absorption and desorption of water within the adhesive is necessary to characterize since the wound site may either be extremely wet or dry depending on the application. The absorption and desorption of water may be affected by the amount of water and glyoxal in the adhesive, which in turn can affect the strength and compliance of the adhesive. The strength and compliance of the adhesive must be adequate to provide for proper wound healing. The altered weight fractions of water and glyoxal will alter the stiffness and strength of the adhesive, which will affect its ability to cover and bind the wound. The gelation of the adhesive during the fabrication process may be influenced by the altered weight fractions of water and glyoxal. The gelation process is sensitive to several variables including the viscosity and pH of the gelatin solution, which will result in either increasing or decreasing the time to cure. A curing time either too long or too short would limit the clinical application of the adhesive.

## **2. BACKGROUND AND LITERATURE REVIEW**

### **2.1 SOFT TISSUE STRUCTURE AND COMPOSITION**

Soft tissues such as organs, blood vessels, muscles, tendons, skin, etc., are made up primarily of connective tissue. Connective tissue can be classified as a composite material, though it is very complex in nature. The extracellular matrix of connective tissue is comprised of fibrils and fibers of collagen and elastin that give the tissue structural integrity and mechanical strength.<sup>9</sup> The interfibrillar matrix, also known as ground substance, is a group of materials found between the fibers and consists of glycosaminoglycans and proteoglycans.<sup>9</sup> The interfibrillar matrix serves to bind the fibers together and prevent interfiber friction.<sup>9</sup> Figure 2.1.1 shows the structural organization of connective tissue. The proportion of matrix present in a specific tissue is related to the tissue function; structural tissue (e.g., skin, bone, or tendon) consists mainly of connective tissue, while tissues with a major metabolic function (e.g., liver or brain) contain little connective tissue.<sup>10</sup> The physical properties of connective tissues result from the chemical structure of the amino acid building blocks that form both fibrous and non fibrous components of connective tissue.<sup>9</sup> There are over 20 amino acid side chains found in the proteins that make up the structural proteins (Table 2.1.1).<sup>9,11</sup> A polypeptide chain is formed when the amino acids bond together by condensation polymerization forming peptide bonds (Figure 2.2.2).<sup>9</sup> Lastly, the sequence of amino acids in a polypeptide chain dictates the conformation of the chain.<sup>9</sup>

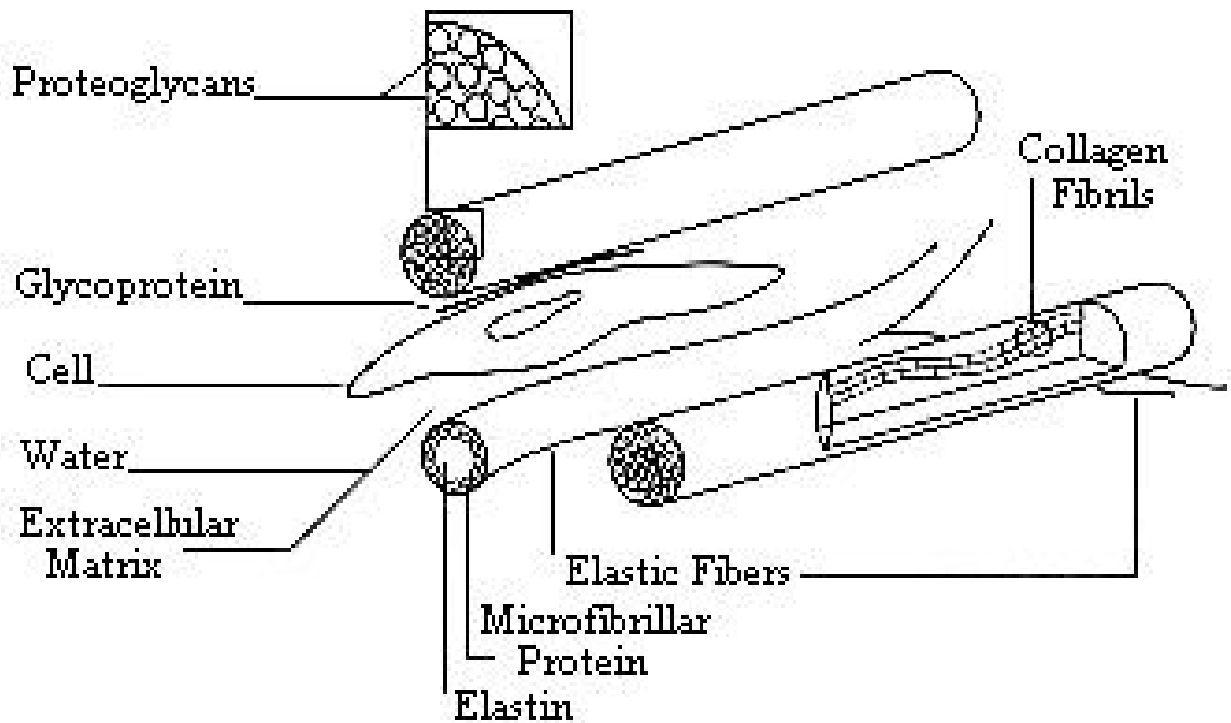


Figure 2.1.1 Structural organization of connective tissue components<sup>9</sup>

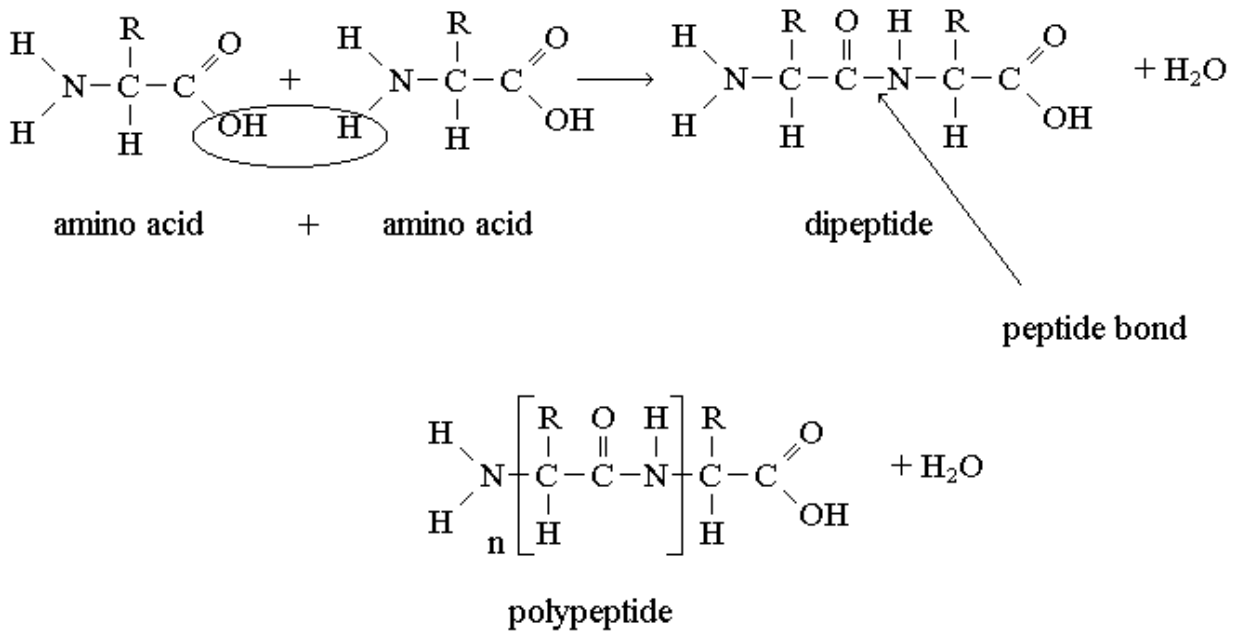


Figure 2.1.2 Condensation polymerization of amino acids forming polypeptide chain<sup>12</sup>

Table 2.1.1 Amino acid R (alkyl) groups<sup>9,11</sup>

Amino Acid	R Group	Amino Acid	R Group
Alanine	-CH <sub>3</sub>	Cysteine	-CH <sub>2</sub> -SH
Methionine	-CH <sub>2</sub> -CH <sub>2</sub> -S-CH <sub>3</sub>	Glycine	-H
Glutamic acid	-CH <sub>2</sub> -CH <sub>2</sub> -CH <sub>2</sub> -C(=O)-O <sup>-</sup>	Aspartic Acid	-CH <sub>2</sub> -C(=O)-O <sup>-</sup>
Hydroxyproline	$  \begin{array}{c}  \text{H}_2\text{C}-\text{CHOH} \\    \quad   \\  -\text{C}-\text{HC} \quad \text{CH}_2 \\    \\  \text{N}  \end{array}  $	Histidine	$  \begin{array}{c}  \text{HC}-\text{N} \\     \quad    \\  -\text{CH}_2-\text{C} \quad \text{CH} \\    \\  \text{N}  \end{array}  $
Arginine	-CH <sub>2</sub> -CH <sub>2</sub> -CH <sub>2</sub> -NH-CH(NH <sub>2</sub> ) <sub>2</sub>	Leucine	-CH <sub>2</sub> -CH(CH <sub>3</sub> ) <sub>2</sub>
Glutamine	-CH <sub>2</sub> -CH <sub>2</sub> -CH <sub>2</sub> -C(=O)-NH <sub>2</sub>	Asparagine	-CH <sub>2</sub> -C(=O)-NH <sub>2</sub>
Lysine	-CH <sub>2</sub> -CH <sub>2</sub> -CH <sub>2</sub> -CH <sub>2</sub> -NH <sub>3</sub> <sup>+</sup>	Serine	-CH <sub>2</sub> OH
Phenylalanine	-CH <sub>2</sub> -C(CH <sub>2</sub> ) <sub>3</sub>	Proline	$  \begin{array}{c}  \text{H}_2\text{C}-\text{CH}_2 \\    \quad   \\  -\text{C}-\text{HC} \quad \text{CH}_2 \\    \\  \text{N}  \end{array}  $
Hydroxylysine	-CH <sub>2</sub> -CH <sub>2</sub> -CH <sub>2</sub> -CH(OH)-NH <sub>3</sub> <sup>+</sup>	Threonine	-CH(OH)-CH <sub>3</sub>
Tyrosine	-CH <sub>2</sub> -C(CH <sub>2</sub> ) <sub>2</sub> -C(OH)	Valine	-CH(CH <sub>3</sub> ) <sub>2</sub>
Isoleucine	-CH <sub>2</sub> -CH <sub>2</sub> -CH(CH <sub>3</sub> )-CH <sub>3</sub>		

### **2.1.1 COLLAGEN**

The most important function of collagen fibrils is to withstand tensile stress. Collagen is composed primarily of glycine, proline, hydroxyproline and alanine amino acid residues, and these account for two of every three amino acid residues in collagen.<sup>9,10</sup> The basic macromolecular unit of collagen is structurally organized by three polypeptide chains coiled in a helix with three residues per turn, and wound into a gentle superhelix about the common molecular axis.<sup>10,11</sup> There are at least ten classifications of collagen, but the three most abundant types of collagens in the mammalian body are type I, II, and III.<sup>13</sup> The various collagens have in common the fact that every third residue in the helical portion is glycine.<sup>12</sup> Type I collagen is the major constituent of bone, tendon, and adult skin.<sup>13</sup> Type II collagen is the main constituent of most tissue that is neither vascularized or innervated, such as cartilage, intervertebral disc, and vitreous humor.<sup>12</sup> Type III collagen is a major component of fetal skin, synovia, placental tissues, uterus, and elastic tissues such as aorta and blood vessels.<sup>13</sup> Type III collagen contains cysteine residues which are not present in the other types of collagen.<sup>13</sup> Types I, III and V collagens are synthesized during wound healing.<sup>12</sup>

### **2.1.2 ELASTIN**

Elastin is a protein found in connective tissue that allows large deformations to take place without permanent damage to the tissue. Elastin exists in high concentrations in tissue where large deformations are functionally necessary, such as the aorta and other blood vessels.<sup>9,13</sup> Elastin is composed primarily of glycine, proline, valine, and alanine amino acid residues.<sup>9</sup> In elastin, tetrapeptide, pentapeptide and hexapeptide repeat units of the amino acids exist.<sup>9</sup>

### 2.1.3 MECHANICAL PROPERTIES OF CONNECTIVE TISSUE

The mechanical properties of connective tissue vary as a result of the collagen and elastic fiber networks as well as the interfibrillar materials.<sup>9</sup> The proportion of elastin and the differentiation of collagen type and content by tissue determines the mechanical strength of the tissue. The behavior of elastin fibers is very similar to an ideal rubber with the elasticity resulting from changes in entropy.<sup>15</sup> However, collagen fibers can have varying degrees of strength and elastic modulus depending on their organization and orientation. Thus, tissues that contain large amounts of elastin such as the aorta can sustain large strains (Figure 2.1.3). Tissues such as tendon; (Figure 2.1.4) which have oriented collagen fiber networks, exhibit an altogether different mechanical response from skin; (Figure 2.1.5), which contains collagen fibers that become oriented upon loading.<sup>9</sup>

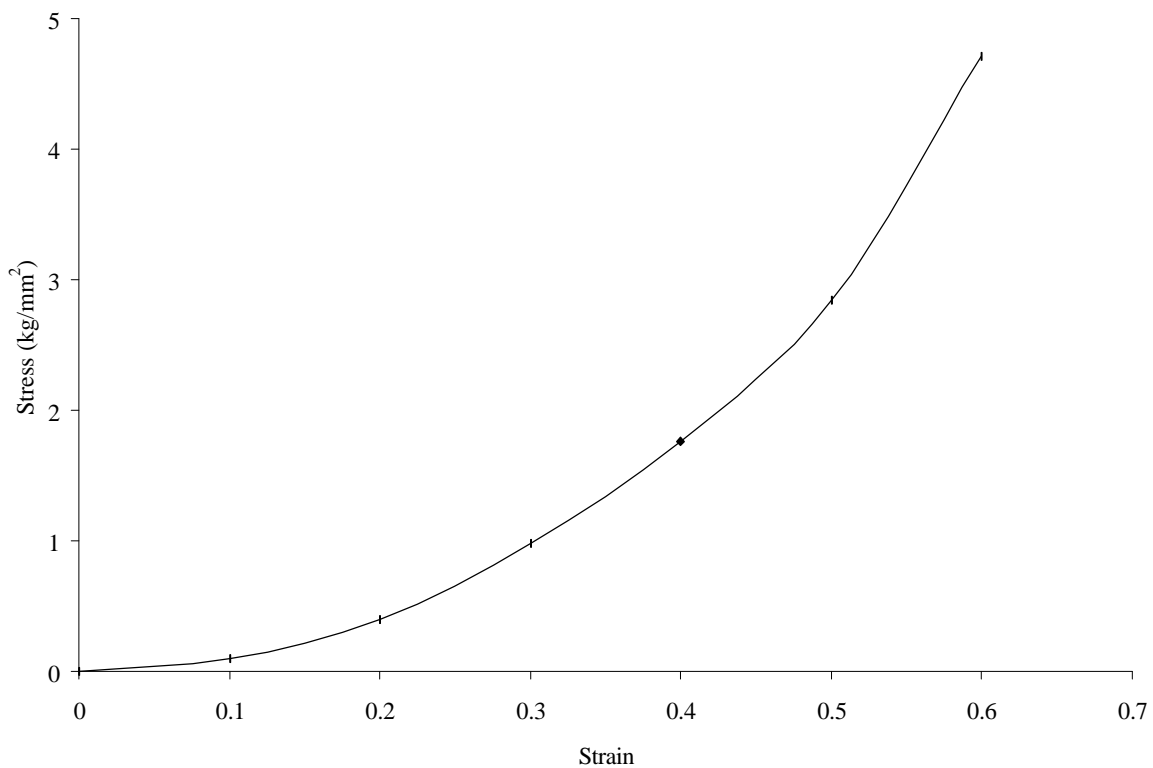


Figure 2.1.3 Stress-strain curve for human thoracic aorta<sup>9</sup>

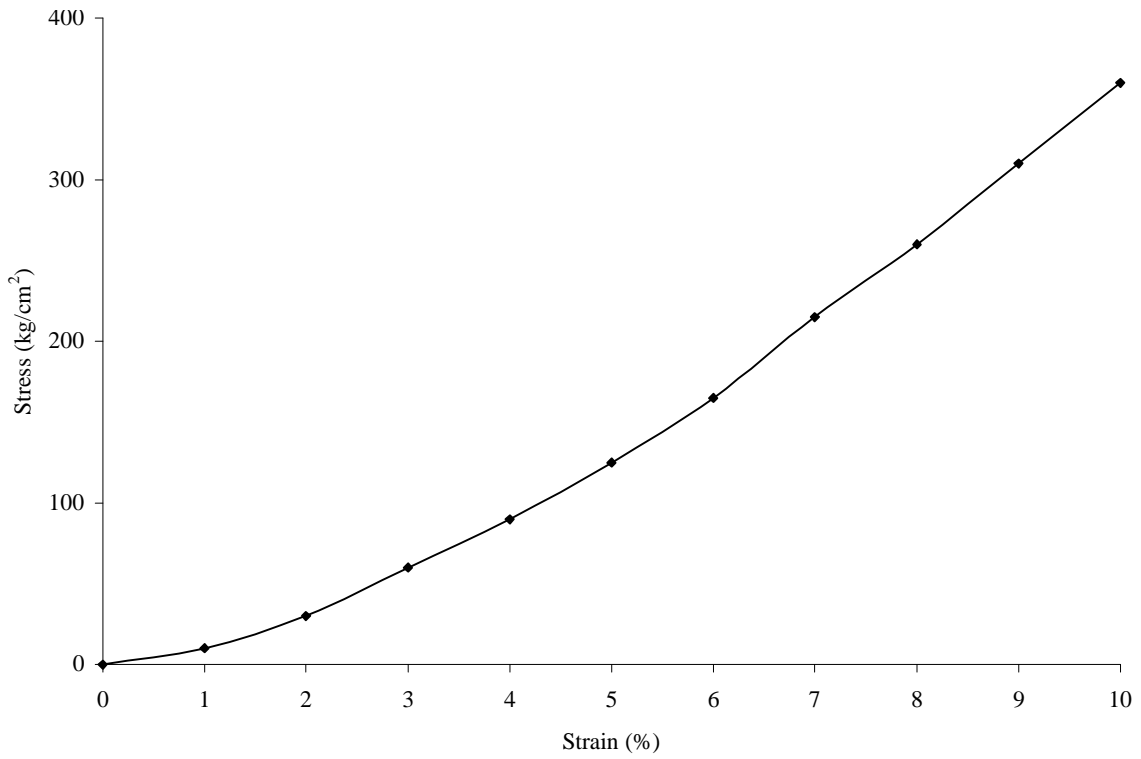


Figure 2.1.4 Stress-strain curve for wet rat tail tendon<sup>9</sup>

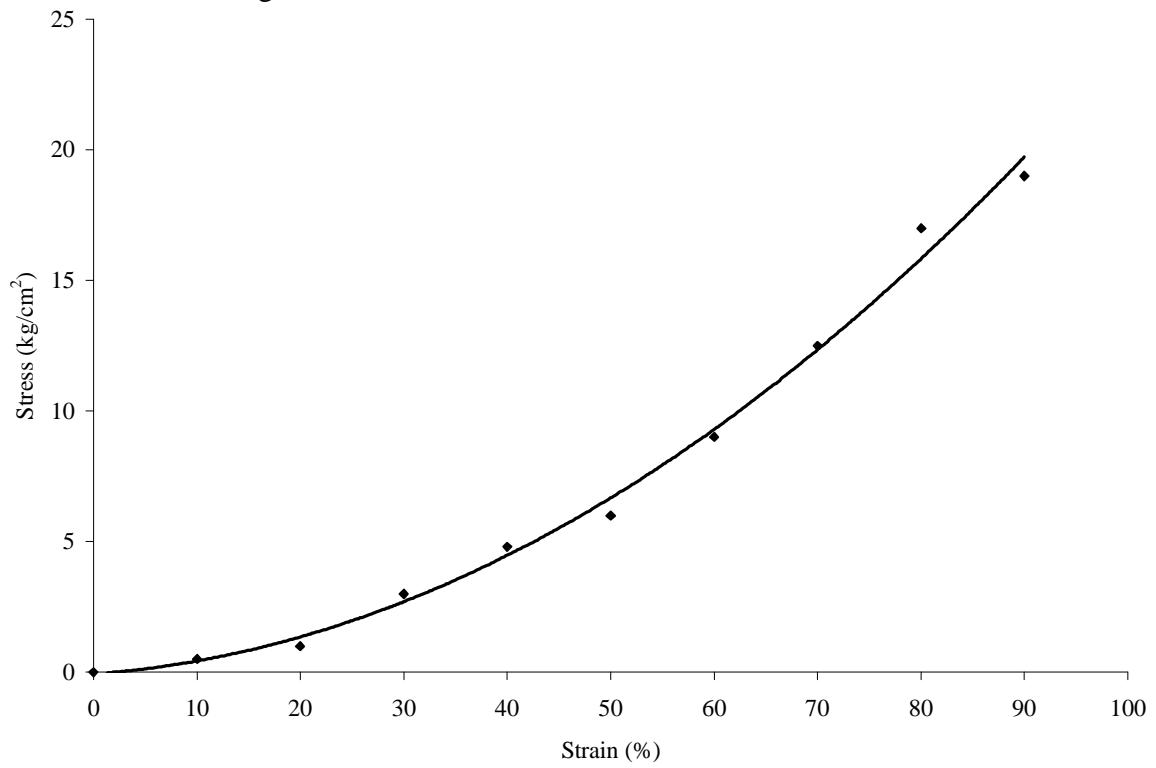


Figure 2.1.5 Stress-strain curve for wet rat back skin<sup>9</sup>



## **2.2 THE USE OF TISSUE ADHESIVES FOR WOUND CLOSURE**

Traditional methods of wound closure utilize sutures and staples, although they have their drawbacks. Foreign body reaction, sinus and granuloma formation, anemia and necrosis can result from sutures or staples being too closely spaced.<sup>16</sup> Suture disruption or degradation leading to wound dishiscence and evisceration, stitch abscess, stitch marks, etc. can also occur.<sup>16</sup> These numerous disadvantages provide the motivation for alternative methods for binding wounds such as using tissue adhesives. The use of tissue adhesives can lead to a rapid and satisfactory wound closure, minimize the time spent in the operating room, as well as reduce the time patients are under anesthesia, the loss of blood and need for transfusions, and other complications that occasionally accompany wound closure.<sup>1</sup> Tissue adhesives require less surgical skill than traditional suturing, and could possibly simplify many surgical procedures.<sup>1</sup> There are several types of tissue adhesives currently available from both synthetic and natural sources. Cyanoacrylate adhesives, fibrin glue, polyurethane adhesives, and several types of gelatin based adhesives have been used experimentally and clinically for wound closure.<sup>1</sup> The ideal soft tissue adhesive must meet many requirements both prior to and after curing, and these objectives are listed in Table 2.2.1.<sup>1-4</sup> An additional advantage sought of a tissue adhesive, though not necessary, would be positive antimicrobial action.<sup>2</sup> Similar to industrial adhesives, the end result of the adhesive bond depends on thickness of adhesive, porosity of the tissue, and flexibility of the adhesive, as well as the rate of degradation.<sup>17</sup>

Table 2.2.1 Requirements of tissue adhesives<sup>1-4</sup>

<b>Before Curing</b>	<b>After Curing</b>
<ol style="list-style-type: none"> <li>1. Sterilizable</li> <li>2. Ease in preparation/mass production</li> <li>3. Adequate shelf life</li> <li>4. Viscous liquid for possible spray or to wet tissue</li> <li>5. Rapidly curable under wet, physiological conditions (pH 7.3, 37<sup>0</sup>C, 1 atm)</li> <li>6. Possess adequate working time</li> <li>7. Locally and systemically nontoxic</li> <li>8. Biocompatible</li> <li>9. Reasonable cost</li> </ol>	<ol style="list-style-type: none"> <li>1. Strong bonding to tissues without producing excess heat from polymerization</li> <li>2. Provide hemostasis</li> <li>3. Tough and pliable</li> <li>4. Locally and systemically nontoxic</li> <li>5. Biocompatible</li> <li>6. Facilitate wound healing</li> <li>7. Biostable union until wound healing</li> <li>8. Resorbable after wound healing/ Insoluble or only slowly soluble in body fluid</li> </ol>

### 2.2.1 GELATIN BASED TISSUE ADHESIVES

Gelatin Resorcinol Formaldehyde (GRF) tissue adhesives were first developed in the mid 1960's by Braunwald and Tatoes and co-workers.<sup>4,5</sup> They were developed as an alternative to cyanoacrylate and polyurethane adhesives since both exhibited poor initial tack and bond strength in the presence of moisture.<sup>4,5</sup> The presence of moisture was found to be much less critical for the bond strength of GRF to tissue compared to cyanoacrylates and polyurethanes.<sup>4</sup> Originally, gelatin and formaldehyde adhesives were formulated, but when bonded to tissue and immersed in Ringer's solution for 18 hours the bond strength decreased and failure occurred within the gelatin phase and not at the tissue junction.<sup>4</sup> Resorcinol was added to the formulation because it instantaneously forms a bond with formaldehyde and therefore improves the moisture resistance of the adhesive.<sup>4</sup> It was also felt that the germicidal nature of resorcinol and formaldehyde was advantageous for the components of a tissue adhesive.<sup>4</sup> In subsequent years, use of formaldehyde in gelatin resorcinol tissue adhesives have been reduced due to toxicity concerns. The tissue adhesives have been cross-linked with mixtures of glutaraldehyde and formaldehyde known as GRFG, and mixtures of difunctional aldehydes such as glutaraldehyde and glyoxal known as GR-DIAL. Since its inception, GRF and its derivatives GRFG and GR-DIAL have found a wide variety of both clinical

and experimental surgical applications and are grouped collectively as hybridized tissue adhesives.<sup>1</sup> GRF has been used experimentally in dogs for sealing wounds of the atrium, ventricle, aorta, lung parenchyma, and to control hemorrhages from the liver and kidney.<sup>4,5</sup> It also has been used clinically for partial nephrectomy, renal trauma and renal allograft rupture.<sup>18</sup> GRFG has been used extensively in clinical applications of acute aortic dissection,<sup>19,21</sup> and experimentally in sealing lung tissue of rabbits.<sup>21</sup> GR-DIAL adhesives have been used experimentally for gluing aortic tissue of pigs and for lung gluing of rabbits and rats.<sup>6,7,19</sup> Studies by Braunwald and Tatoes found adequate bonding of GRF for sealing the atrium and ventricle, lung parenchyma, and thoracic aorta, but not for sealing divided bronchial stumps using the dog as an animal model.<sup>4,5</sup> Localized tissue irritability was evidenced in the sealing of blood vessels and bronchi but was not a factor in sealing parenchymous tissues of the heart and lung, where no systemic toxicity or localized areas of tissue irritation were found.<sup>4</sup> In a second study by Braunwald and Tatoes, the bond strength of GRF used for liver and kidney hemostasis of dogs was found to be satisfactory and no evidence of systemic toxicity was observed.<sup>5</sup> Horznek reports that in clinical use of GRF for partial nephrectomy, renal trauma and renal allograft rupture, there have been satisfactory results and good tissue tolerance.<sup>18</sup> In clinical treatment of aortic dissection, good tissue tolerance of GRFG and good repair was found.<sup>7</sup> A study over two months on the effects of GRFG on vessel morphology of rats conducted by Walker *et al.* found that there was no evidence of wound breakdown, infection or necrosis, and no GRFG was visible 2 months postoperatively, suggesting complete biodegradation.<sup>3</sup> Studies on rabbits by Ennker *et al.* have found adequate bonding using GR-DIAL and the resin demonstrated better adhesive strength than GRF on humid surfaces. GR-DIAL also demonstrated adequate biocompatibility, gradual disintegration, and bioresorption.<sup>6,7</sup> In a study conducted by Wertzel; *et al.*, the GR-DIAL proved effective in tight bronchial stump closure of rats, with no local infection or necrosis. Complete resorption (degradation) of the adhesive was also noted 120 days postoperatively.<sup>22</sup> Limited work has also been conducted on gelatin Poly (L-glutamic acid) (PGA) mixtures cross-linked with water-soluble carbodiimide (WSC).<sup>1,23-26</sup>

## 2.3 COMPONENTS OF HYBRIDIZED TISSUE ADHESIVES GELATIN

### 2.3.1 GELATIN

Gelatin is classified as a derived protein because it is produced by denaturing, drying and extraction of collagen.<sup>10,11</sup> The denaturing process of collagen involves the destruction of the triple helix structure of collagen by heating.<sup>10,11,27</sup> Gelatin can be derived from either an acid treated precursor such as pork skin (Type A), or alkaline treated precursor such as cattle hide and bone (Type B).<sup>27</sup> The precursor material determines the specific amino acid content of the gelatin, with the following amino acids making up the largest content: Proline, Hydroxyproline, Glycine, Glutamic Acid, and Alanine.<sup>10,27</sup> In dilute solutions, the quality of gelatin is quantified by Bloom strength. For Bloom strength testing, a water solution of 6.67% gelatin is prepared in a 150 ml wide mouth glass bottle, and chilled in a water bath at 10<sup>0</sup>C for 17 hours. Using a Bloom gelometer or Texture Analyzer, the force, in grams, required to impress a plunger 12.7 mm in diameter, 4 mm deep into the gelatin sample is measured as the Bloom strength.<sup>10,27</sup> Gelatin with Bloom strength ranging between 50 and 300 Bloom Grams in a variety of particle sizes (meshes) is available commercially.<sup>27</sup> Gelatin is used commercially in a wide range of applications, from uses in food to adhesives in book binding and furniture making, photographic uses, and pharmaceutical applications.<sup>10,27</sup> A gelatin gel results from a process known as gelation. Gelation occurs when the gelatin aggregates and sets, with an increase in viscosity with increasing time as seen in Figure 2.3.1.<sup>10</sup> Upon cooling of gelatin solutions, a molecular network results with a partial return of the gelatin molecules to the triple helix collagen structure.<sup>10</sup> Factors affecting gelation are thermal history, molecular weight, pH, and initial viscosity of the gelatin solution.<sup>10</sup> When cooling of gels occurs very rapidly, a fine network with little order results, whereas if a gel is cooled rather slowly, a courser network with more inter-chain bonding results.<sup>10</sup> The viscosity of a concentrated gelatin solution is dependent on pH, temperature, and concentration. On a curve of measured viscosity versus pH, the viscosity is a minimum at the isoionic point, which is the point when there are no colloidal ions other than hydrogen and hydroxyl ions.<sup>10,11</sup> When the pH is raised or lowered the net charge increases and causes the polypeptide chains to unfold increasing the viscosity.<sup>10</sup> The initial viscosity is a maximum in gelatin solutions with pH of 3 and 10.5.<sup>10</sup> The viscosity increases exponentially with gelatin content, and as the gelatin concentration is increased the effect

of pH on viscosity is less than the effect for more dilute solutions.<sup>10</sup> The viscosity above 40°C decreases exponentially with temperature.<sup>10</sup> In conclusion the process of gelation is subject to many variables which affect the overall structure of the formed gel and is somewhat dependent on the test methods used to identify it.

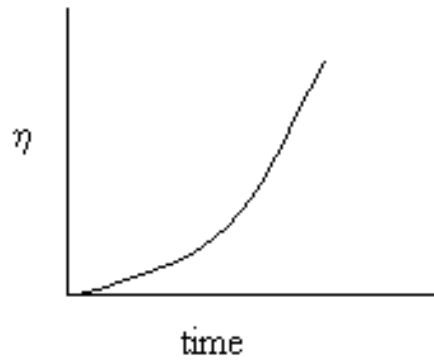


Figure 2.3.1 Characteristic shape of curve for viscosity ( $\eta$ ) versus time as gelatin solution is cooled<sup>10</sup>

### 2.3.2 RESORCINOL

Resorcinol may be known by several different names such as resorcin, 1,3 dihydroxy benzene, hexahydroresorcinol or 1,3-Cyclohexandiol (Figure 2.3.2).<sup>28</sup> Commercially, resorcinol is used extensively as in resorcinol/formaldehyde resin for wood adhesives and to improve adhesion of rubber to reinforcing materials in tire manufacture.<sup>28</sup> It is considered to be slightly to moderately toxic and a mild skin irritant which raises biocompatibility concerns.<sup>28</sup> It is easily absorbed by skin and mucous and is eliminated primarily from the body by the kidneys.<sup>28</sup> Resorcinol is often used as an ingredient in over the counter treatments of dandruff, acne, and scabies due to its antiseptic, keratinolytic action with a minimum concentration of 2%.<sup>28</sup> In 1991, it was generally recognized as safe by the FDA for use in over the counter acne treatments.<sup>28</sup> Resorcinol is also used as a coupling agent in hair dyes.<sup>28</sup>

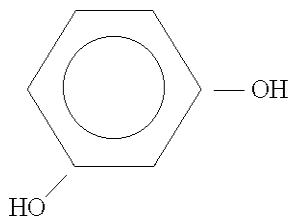


Figure 2.3.2 Structure of Resorcinol<sup>28</sup>

### 2.3.3 CROSSLINKING OF HYBRID TISSUE ADHESIVES WITH ALDEHYDES

Aldehydes such as formaldehyde and dialdehydes such as glutaraldehyde and glyoxal known as difunctional aldehydes have been used as cross-linking agents of proteins and tissue adhesives; (Figure 2.3.3). Aldehydes produce inter and intramolecular cross-linking in proteins by covalent bonding via Schiff base formation with the amino groups; (Figure 2.3.4).<sup>8,28</sup> Gelatin cross-linked in the solution state generally leads to weaker gels because the covalent cross-links interfere with the freedom of the polypeptide chains to adopt the conformation for the gel structure.<sup>10</sup> If gelatin gels are cross-linked after gelation the gels have much higher strength.<sup>10</sup> Formaldehyde, glutaraldehyde and glyoxal bond with resorcinol by polycondensation reactions; (Figure 2.3.5).<sup>1,7,29</sup> Although these three aldehydes have considerable antimicrobial effects, there is considerable concern about their toxicity.<sup>4,5,8</sup> Formaldehyde is considered the most toxic of the three being known to be both carcinogenic and mutagenic, and glyoxal is the least toxic.<sup>7</sup> Formaldehyde and glutaraldehyde are used extensively as fixative agents and in leather manufacture because of their ability to cross-link proteins.<sup>8</sup>

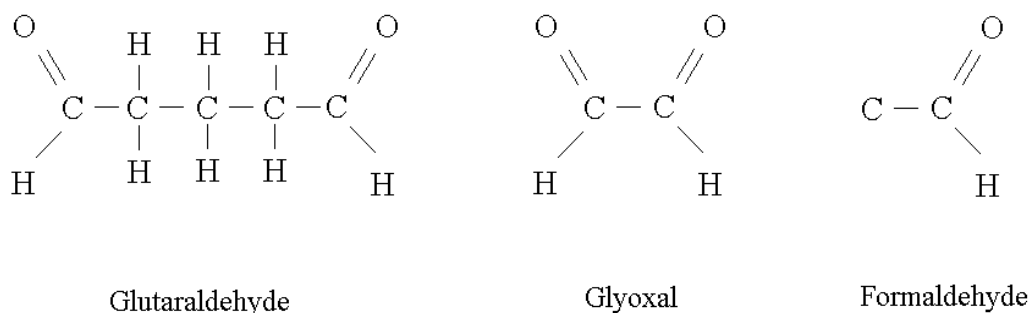


Figure 2.3.3 Structure of aldehydes

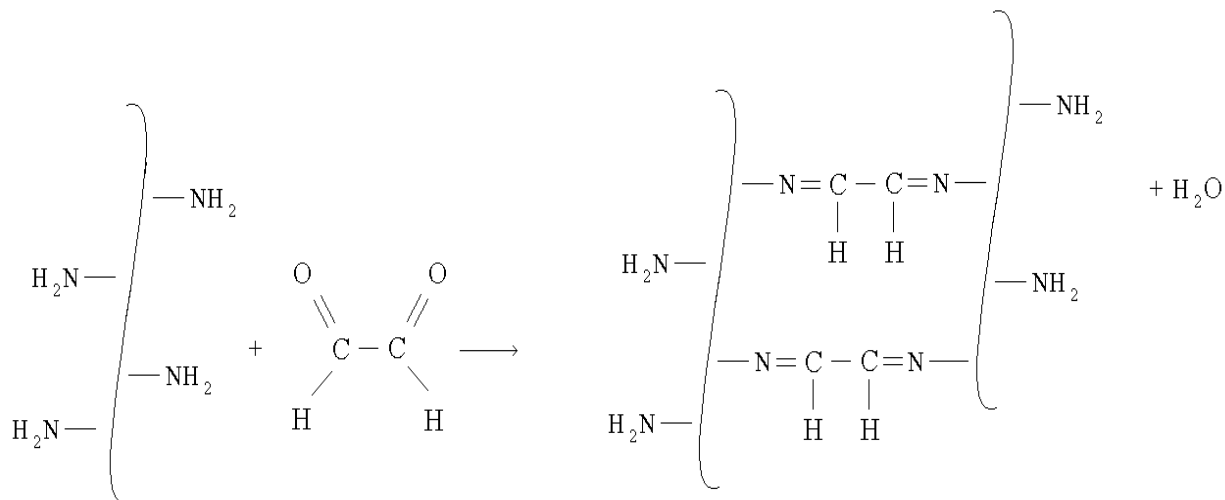


Figure 2.3.4 Idealized representation of cross-linking of protein by glyoxal<sup>1,28</sup>

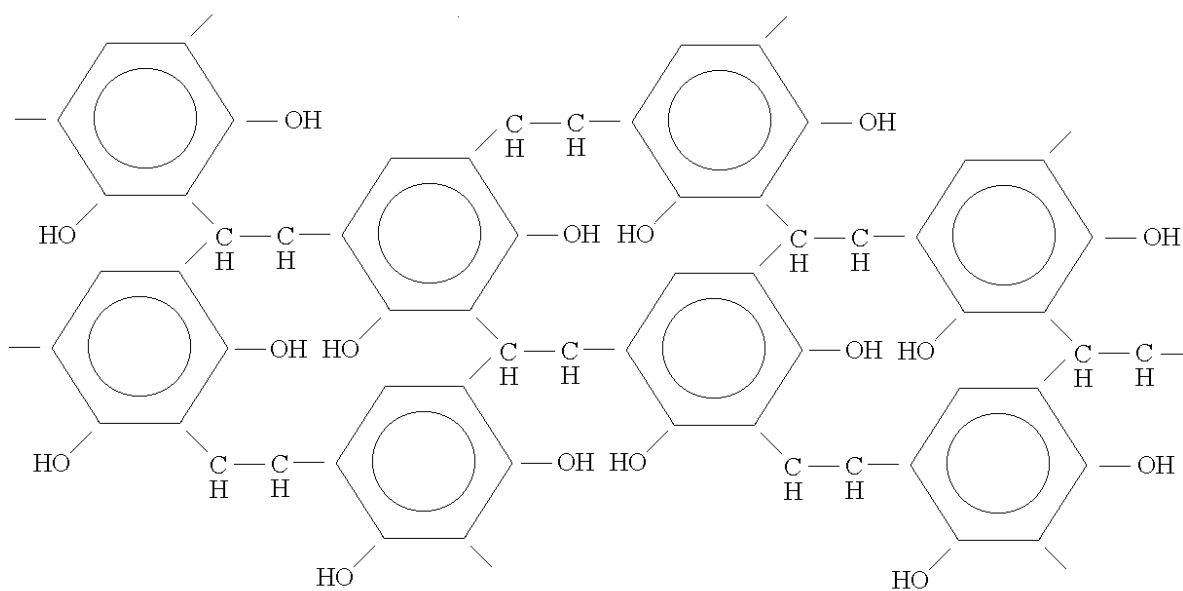


Figure 2.3.5 Resin formed from condensation reaction of glyoxal and resorcinol<sup>29</sup>



### 2.3.4 MECHANISMS OF DEGRADATION

Hybridized tissue adhesives are believed to be biodegradable because gelatin can be dissolved and digested by proteolytic enzymes. Gelatin may be degraded *in vivo* by proteolytic enzymes such as collagenase.<sup>13</sup> Collagenase is a naturally occurring enzyme present in healing wounds.<sup>30</sup> However, chemical cross-linking such that occurs by aldehydes decelerates the degradation rate of gelatin.<sup>2</sup> The *in vitro* degradation rate of collagen cross-linked with formaldehyde, glutaraldehyde and glyoxal was found to increase exponentially with increased molecular weight between cross-links; (Figure 2.3.6).<sup>30</sup>

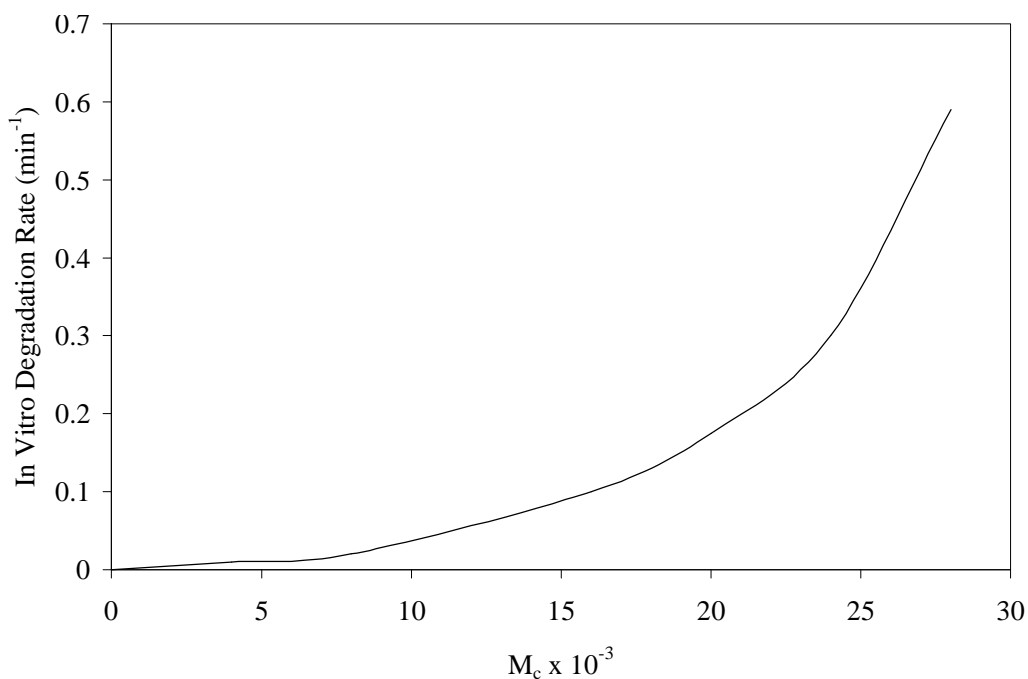


Figure 2.3.6 In vitro degradation rate of collagen as a function of molecular weight between cross-links<sup>30</sup>

## 2.4 MEASUREMENT OF pH AND GELATION TIME OF TISSUE ADHESIVES

The pH and gelation time of tissue adhesives need to be assessed because the gelation process of the gelatin component is very sensitive as mentioned in section 2.3.1. The setting time of gelatin is pH dependent with minima in the pH/gelation time curves at pH 4.5-5.5 for alkali processed gelatins and pH of 6 for acid processed gelatins.<sup>10</sup> However, the effects of resorcinol and glyoxal on the pH and setting time of the tissue are not known. The speed and completeness of the chemical cross-linking of gelatin with an aldehyde are also pH dependent.<sup>5</sup> According to Shaunstein *et al.*, the quantity of bound formaldehyde in collagen rises steeply with increasing pH<sup>8</sup>, and is most likely analogous for other aldehydes. In the clinical application of tissue adhesives, setting time can be considered a measure of the working time available to the clinician and how instantaneously the tissues may be bonded together. Otani and coworkers using gelatin-Poly(L-glutamic acid) gels cross-linked with water soluble carbodiimide (WSC), measured the gelation (setting) time by measuring the duration of time for the solution under constant stirring to stop following the addition of the cross-linking agent.<sup>23-25</sup>

## 2.5 DRYING AND SWELLING OF TISSUE ADHESIVES

The drying and swelling of tissue adhesives need to be assessed because of the wide range of applications *in vivo*. For example, a tissue adhesive applied to the surface of the skin is exposed to relatively dry conditions on one side at temperatures close to body temperature (37°C), but if used as a surgical adhesive, it would be exposed to a comparably wet environment at 37°C. The drying or desorption of water can be attributed to diffusion of water from the bulk of the adhesive to the surface, followed by evaporation. The absorption of water is attributed to diffusion resulting in swelling of the adhesive. Absorption or desorption of water in the adhesive can be expressed according to Fick's law of diffusion for the rate of change of concentration at any point.<sup>31</sup>

$$\frac{dc}{dt} = D \frac{d^2c}{dx^2} \quad (2.5.1)$$

Where  $c$  represents the concentration,  $x$  the position in the material,  $t$  the time, and  $D$  the diffusivity constant. For a plane sheet of uniform and constant thickness  $L$  with constant and uniform initial concentration, Figure 2.5.1, the total amount of water entering or leaving the adhesive at time  $t$  is given by:

$$\frac{M_\infty - M_t}{M_\infty} = \frac{8}{\pi^2} \exp\left(-\frac{\pi^2 Dt}{L^2}\right) \quad (2.5.2)$$

where  $M_\infty$  is the mass of water that has entered or left the adhesive at infinite time, and  $M_t$  is the mass of water that has entered or left the adhesive at time  $t$ .<sup>31</sup> An example plot of equation 2.5.2 is given in Figure 2.5.2.

The degree of swelling can also be explained using Flory-Rehner's classical theory of swelling relating the molecular weight between cross-links to the degree of swelling.<sup>32-34</sup> The equation derived by Flory and Rehner is given by:

$$v_{2m}^{5/3} \cong \frac{2rV_s}{M_c \left( \frac{1}{2} - c_1 \right)} \quad (2.5.3)$$

The molecular weight between cross-links is represented by  $M_c$ , the polymer density by  $\rho$ , and the volume fraction of polymer to the swollen polymer network  $\frac{V}{V_0}$  is represented by  $v_{2m}$ ,  $V_s$  is the molar volume of the solvent, and  $c_1$  is an interaction parameter for the polymer and solvent. From this equation, if the molecular weight between cross-links of a polymer is decreased, it is expected that its resistance to swelling will increase.

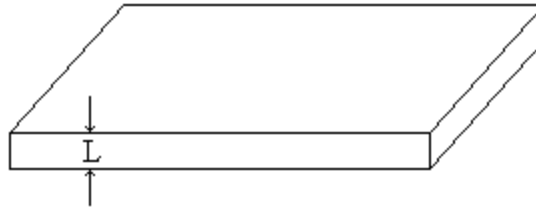


Figure 2.5.1 Sheet of thickness  $L$  used for diffusion equations<sup>31</sup>

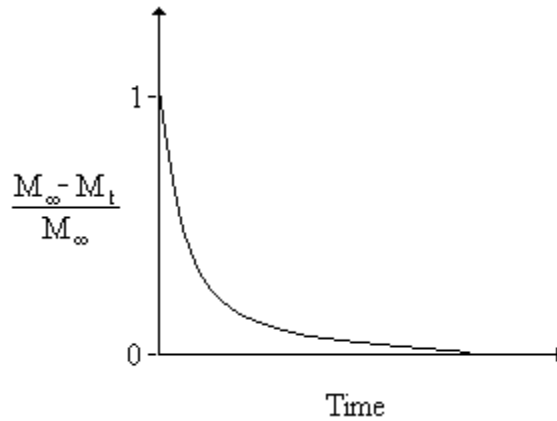


Figure 2.5.2 Example plot of equation 2.5.2<sup>31</sup>

## 2.6 THERMAL ANALYSIS

The transitional characteristics of the adhesives can be characterized using Differential Scanning Calorimetry (DSC), and Dynamic Mechanical Spectroscopy (DMS), while Thermogravimetric Analysis (TGA) can assess the thermal stability. Differential Scanning Calorimetry (DSC) is used to identify transitional characteristics of polymers such as the glass transition temperature ( $T_g$ ), crystallization, and melting temperature. Dynamic Mechanical Spectroscopy is used to identify the onset of molecular motion, typical of  $T_g$ , by measuring the changes in the components of complex dynamic modulus with temperature. The transitional characteristics of gelatin resorcinol dialdehyde tissue adhesives may be sensitive to the additions of water and the cross-linker glyoxal. The water component of the adhesives may act as a plasticizer because of the amount of hydrogen bonding potential to the hydroxyl and acid functionalities of the resin. In a polymer, a plasticizer lubricates the polymer chains by separating the chains, thus lowering the  $T_g$  and making the polymer more flexible and compliant.<sup>35</sup> The depression of  $T_g$  depends on the amount of plasticizer present.<sup>35</sup> The depression of  $T_g$  by the addition of plasticizer can be predicted according to the Fox-Flory equation.<sup>35-38</sup>

$$\frac{1}{T_g^{new}} = \frac{w_p}{T_g^p} + \frac{w_l}{T_g^l} \quad (2.6.1)$$

The  $T_g$  of the plasticized polymer is represented by  $T_g^{new}$  and the  $w_p$  and  $w_l$  represent the weight fractions of polymer and liquid, and  $T_g^p$  and  $T_g^l$  are the respective glass transition temperatures for the polymer and plasticizer. Addition of cross-linker has an opposite effect on the glass transition temperature. Cross-linking restrains the mobility and maintains the arrangement of the polymer chains in the network by providing anchoring points; (Refer to Figure 2.6.1).<sup>35</sup>

In the literature, it has been observed that in hydrophilic polymers such as gelatin, water crystallizes only partially when cooled.<sup>37,39</sup> According to Rault *et al.*, bound water does not crystallize when the temperature is decreased but unbound water does crystallize.<sup>39</sup> Figure 2.6.2 illustrates the possible incidence of unbound water in the bulk adhesive. According to Rault *et al.*, crystallization of water only occurs when the concentration of water exceeds a critical

concentration in the polymer.<sup>39</sup> Below the critical concentration of water, the glass transition temperature follows the Fox-Flory equation, however, above the critical concentration the  $T_g$  is constant and equal to the melt temperature of ice and is known as the  $T_g$  regulation effect.<sup>39</sup> Ponomariova and coworkers, utilizing DSC to analyze Polyacrylamide gels, found the critical concentration of water increases with the cross-link density and concluded that crystallization of water appears at lower temperature in highly cross-linked materials.<sup>38</sup> Using DSC, Apostolov and co-workers found that the critical concentration for water in gelatin was 30%, but obtained mixed results for gelatin with altered cross-linker content.<sup>37</sup> In another study using DSC, Tenhu *et al.* found that gelatin samples cross-linked with glutaraldehyde at 50<sup>0</sup>C contained more non-crystalline (bound) water than untreated samples.<sup>40</sup> It should be noted that for the studies on cross-linked gelatin, the conditioning and methods of fabrication of the samples varied, and the adhesive will be very sensitive to these differences. For gelatin containing large concentrations of water it is recommended to use Dynamic Mechanical Spectroscopy (DMS) since DSC can not be used because the  $T_g$  is hidden by the melting peak of ice.<sup>37</sup>

Thermogravimetric analysis is used to measure the thermal stability of a polymer by measuring weight changes as a function of temperature and time.<sup>41</sup> Apostolov and coworkers investigated the thermal stability of water in cross-linked gelatin using TGA and concluded that crystallized water leaves the system by evaporation at relatively low temperatures of 25-100<sup>0</sup>C and noncrystallized water leaves the system over the entire temperature interval of 25<sup>0</sup>C to 300<sup>0</sup>C.<sup>37</sup> Farikov and coworkers, using dried cross-linked gelatin films, measured the loss of water from the system using TGA, and concluded that the water bound by hydrogen bonds to the gelatin leaves the system at temperatures of 150-170<sup>0</sup>C.<sup>42</sup>

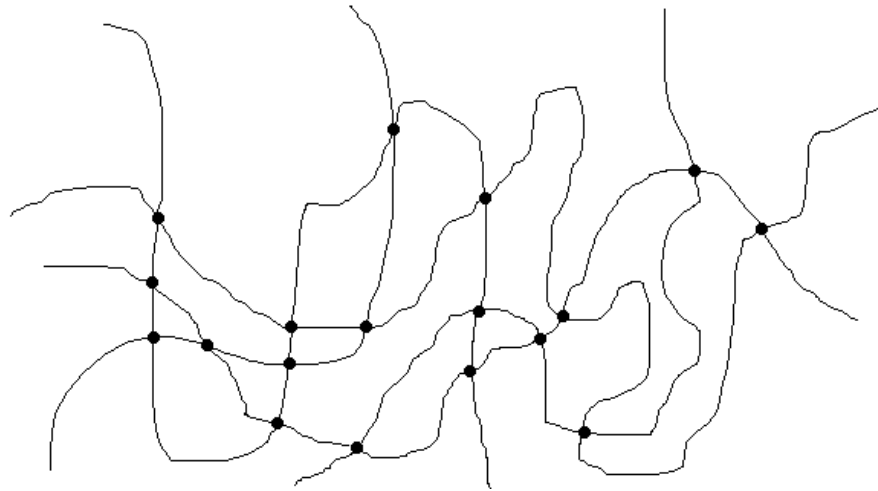


Figure 2.6.1 Illustration of cross-linked chains in a network polymer

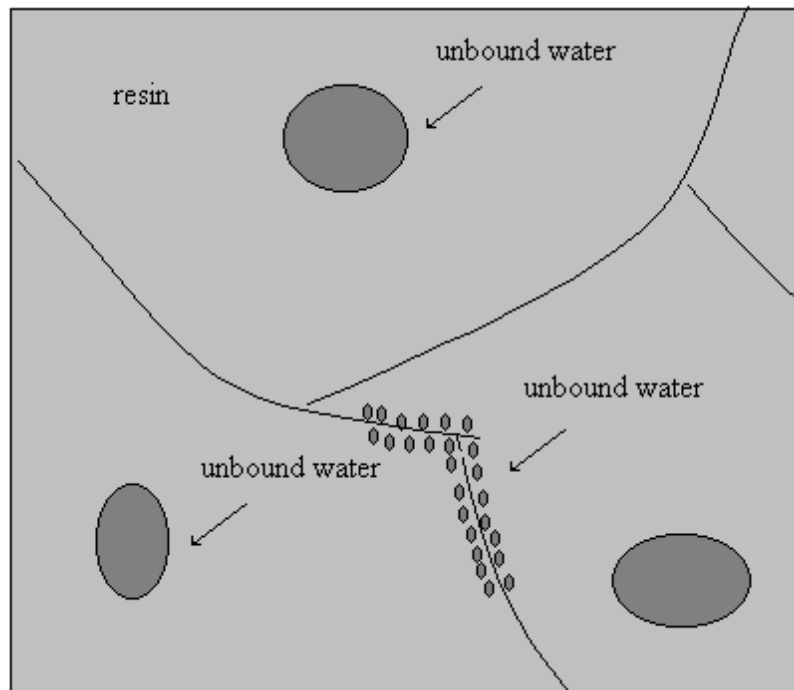


Figure 2.6.2 Illustration of possible existence of bound and unbound water in the bulk adhesive

## **2.7 TENSILE TESTING**

Stress-strain tensile testing is used to assess the strength and elastic modulus of polymers. For tissue adhesives, it is important that they be relatively strong and ductile to match the properties of the variety of tissues that may be bonded. If the strength and ductility of the tissue adhesive are not adequate, failure of the tissue adhesive may occur and wound closure may not be attainable. However, if the strength of the adhesive is much greater than the bonded tissue, when a force is applied, tearing of the wound or surrounding tissue may occur. The elastic modulus, the strength, and strain at break of the adhesive may be altered by addition of plasticizer and cross-linking agent.



## 2.8 STRESS RELAXATION

Stress relaxation tests are utilized to characterize the visco-elastic behavior of materials. Both connective tissue and many polymers such as gelatin based tissue adhesives exhibit visco-elastic behavior.<sup>9</sup> Under constant deformation the stress within the materials relaxes with time, Figure 2.8.1. Differences in the visco-elastic behavior of tissue adhesives may be observed as result of variations in plasticizer and cross-linker content. Plasticizer may increase the viscous response, while cross-linking may increase the elastic response. Stress relaxation can be modeled simplistically using the Maxwell model consisting of a spring and dashpot in series, Figure 2.8.2.<sup>43</sup> For a single Maxwell unit, the stress strain relation for the spring element is:

$$\mathbf{s}_s = Ee_s \quad (2.8.1)$$

where E represents the elastic modulus and  $e_s$  represents the strain of the spring and  $\sigma_s$  represents the stress of the spring. The stress strain relationship for the dashpot is:

$$\mathbf{s}_d = \mathbf{h} \frac{de_d}{dt} \quad (2.8.2)$$

where  $\eta$  represents the viscous component, and  $e_d$  represents the strain of the dashpot. Equation 2.8.1 can now be rewritten given the physical restraints:  $\mathbf{s}_s = \mathbf{s}_d = \mathbf{s}$  and  $e_d + e_s = e$  as:

$$\frac{d\mathbf{s}}{dt} = E \frac{de}{dt} \quad (2.8.3)$$

Combining with equation 2.8.2 yielding:

$$\frac{de}{dt} = \frac{1}{E} \frac{d\mathbf{s}}{dt} + \frac{\mathbf{s}}{\mathbf{h}} \quad (2.8.4)$$

For a stress relaxation experiment, the strain is held constant, therefore:

$$\frac{de}{dt} = 0 \text{ and } \frac{1}{E} \frac{d\mathbf{s}}{dt} + \frac{\mathbf{s}}{\mathbf{h}} = 0 \quad (2.8.5)$$

Equation 2.8.3 can now be written as:

$$\frac{d\mathbf{s}}{\mathbf{s}} = -\frac{E}{h} dt \quad (2.8.4)$$

Integrating equation 2.8.4 using  $\mathbf{s} = \mathbf{s}_0$  at time  $t=0$  becomes:

$$\mathbf{s} = \mathbf{s}_0 \exp\left(\frac{-E}{h} t\right) \quad (2.8.5)$$

Substituting  $t = \left(\frac{h}{E}\right)$

$$\mathbf{s} = \mathbf{s}_0 \exp\left(\frac{-t}{\tau}\right) \quad (2.8.6)$$

For a better approximation in modeling stress relaxation, multiple Maxwell units linked in parallel can be used, see Figure 2.8.3. For  $n$  Maxwell units in parallel the stress can be modeled as:

$$\mathbf{s}(t) = e \sum^n E_n \exp\left(\frac{-t}{\tau_n}\right) \quad (2.8.7)$$

Replacing the Young's (elastic) modulus ( $E$ ) with  $f(\tau)$  which is a distribution function, equation 2.8.7 can be written as:

$$\mathbf{s}(t) = \mathbf{s}_\infty + e \int_0^\infty f(\tau) \exp\left(\frac{-t}{\tau}\right) d\tau \quad (2.8.8)$$

Normalizing the stress and considering two Maxwell units in parallel the equation can be written as:

$$\frac{\mathbf{s}}{\mathbf{s}_0} = \mathbf{s}_\infty + A_1 \exp\left(\frac{-t}{\tau_1}\right) + A_2 \exp\left(\frac{-t}{\tau_2}\right) \quad (2.8.9)$$

where  $\mathbf{s}_\infty$  is the stress at infinite time and  $A_1$  and  $A_2$  are constants.

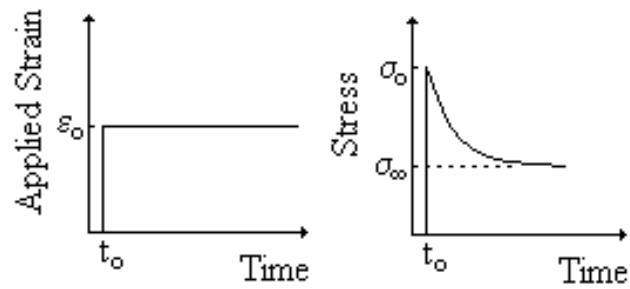


Figure 2.8.1 Illustration of stress relaxation resulting from constant applied strain<sup>43</sup>

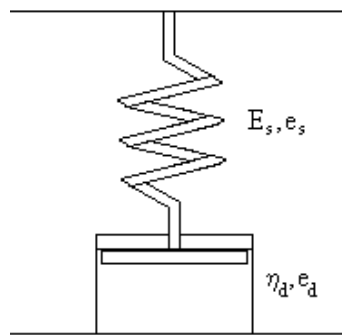


Figure 2.8.2 Maxwell model – spring and dashpot in series<sup>43</sup>

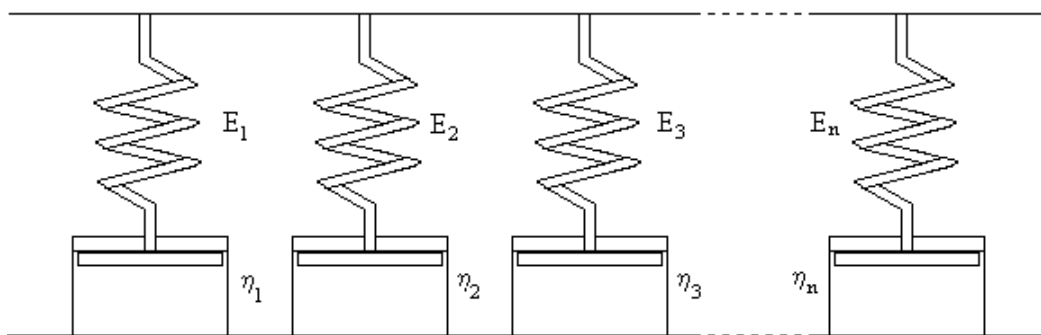


Figure 2.8.3 Multiple Maxwell units in parallel used to simulate more complicated stress relaxation responses<sup>43</sup>

## 2.9 ADHESION

### 2.9.1 THEORIES OF ADHESION

Adhesion occurs when the adhesive and adherend are brought into intimate molecular contact at the interface.<sup>44</sup> Mechanical interlock, diffusion, electronic forces, and adsorption theories can describe the nature of the molecular forces at the interface that allow the stress to be transferred from one adherend to the other.<sup>44,45</sup> Adsorption theory postulates that van der Waals forces and hydrogen bonding between the molecules of the adhesive and substrate should be adequate for good adhesion provided that there is good interfacial contact.<sup>45</sup> In addition to the van der Waals forces acting on the interfacial bond, chemisorption may occur which is bonding by primary ionic, covalent, and metallic bonds known as primary bonding.<sup>44</sup> Hydrogen bonding between gelatin and tissue is implicated as an adhesion mechanism for gelatin based tissue adhesives such as GRF.<sup>4,5</sup> Mechanical interlock theory of adhesion postulates that penetration of the adhesive into the surface irregularities of the substrate result in a mechanical interlocking of the materials.<sup>44</sup> The electronic theory is described as the development of an electrical charge double layer at the interface of a bond as a result of the differences in electron band structures of the adhesive and adherend.<sup>44</sup> The diffusion theory is described as the mutual diffusion of polymer molecules across the interface, provided there is adequate chain mobility and mutual solubility.<sup>44</sup> It is thought that in most adhesive bonds, more than one adhesion mechanism is responsible for strong adhesion.

## 2.9.2 WETTING AND CONTACT ANGLE MEASUREMENTS

The formation of an interface between the adhesive and the adherends occurs by wetting, and this process can be divided into adhesion wetting and spreading wetting. Adhesion wetting occurs when the interface area of a solid and a liquid increases and both the liquid-gas and solid-gas interfacial areas are decreased.<sup>45,46</sup> Spreading wetting occurs when the area of solid-liquid and liquid gas interfaces increases and the solid-gas interface is decreased.<sup>45,46</sup> In order for strong adhesion to occur between tissue adhesive and a wound site and tissue adhesive, adequate wetting must occur. The extent of wetting can be determined by measuring the equilibrium contact angle. The contact angle is defined as the angle formed between the solid liquid interface and the liquid gas interfaces on an ideally smooth, planar undeformable, homogenous surface, Figure 2.9.1.<sup>45-48</sup> The spreading equilibrium contact angle is calculated by the scalar addition of the interfacial tensions between the solid, liquid and gas by Young's equation<sup>45-48</sup> and is given by:

$$\mathbf{g}_{SL} + \mathbf{g}_{LG} \cos \mathbf{q} - \mathbf{g}_{SG} = 0 \quad (2.9.1)$$

$$\mathbf{g}_S - \mathbf{g}_{SG} = \mathbf{p}_{SG} \quad (2.9.2)$$

The surface tension of the solid-liquid, liquid gas, and solid-gas interfaces are given by  $\mathbf{g}_{SL}$ ,  $\mathbf{g}_{LG}$ , and  $\mathbf{g}_{SG}$  respectively. The surface tension of the solid in equilibrium with its own vapor is given by  $\mathbf{g}_S$ , and the spreading pressure is given by  $\mathbf{p}_{SG}$ . The effects on the contact angle from spreading pressure are considered low when measured values of the contact angle  $\mathbf{q}$  are large. Similarly Dupre' derived an equation relating the interfacial surface tension to the work of adhesion<sup>45-48</sup> given by:

$$W_a = -\frac{\Delta G}{A} = \mathbf{g}_{LG} + \mathbf{g}_{SG} - \mathbf{g}_{SL} \quad (2.9.3)$$

Combining the equations of Young and Dupre',<sup>45-48</sup> the contact angle is related to the surface tension of the liquid gas interface and is given by:

$$W_a = \mathbf{g}_{LG} (1 + \cos \mathbf{q}) \quad (2.9.4)$$

According to the Young-Dupre' equation, a zero contact angle is observed when the forces of attraction between the liquid and solid are greater than the forces within the liquid. A measurable contact angle is detected when the liquid adheres to itself more than to the solid surface.<sup>46</sup> The solid surface is considered partially wetted if the contact angle is finite but, completely wetted if the contact angle is zero.<sup>46</sup> In conclusion, in order for wetting of a solid to occur it is advantageous that the liquid have a lower surface tension than the solid.

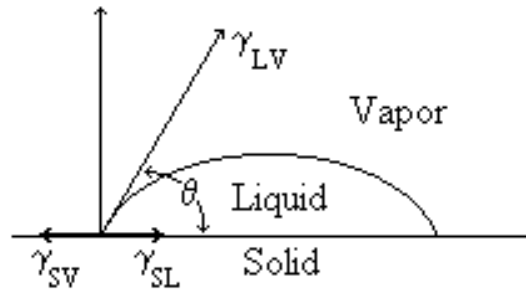


Figure 2.9.1 Representation of a liquid wetting a solid surface and contact angle formed

### 2.9.3 DETERMINATION OF SURFACE TENSION FROM CONTACT ANGLE MEASUREMENTS

The surface tension of a solid can not be directly measured, however, several indirect methods have been developed.<sup>47</sup> The harmonic-mean method is regarded as an accurate technique for determining the surface tension of a solid from contact angle measurements.<sup>47</sup> The harmonic-mean method utilizes the contact angle measurements of two liquids independently tested on the substrate. Water and methylene iodide are two advantageous liquids to use for contact angle measurements since water is polar in nature while methylene iodide is not, Table 2.9.1.<sup>47</sup> The harmonic mean equation<sup>47</sup> takes into account the polar and dispersive (nonpolar) molecular force contributions to the surface tension and is given by:

$$\mathbf{g}_{SL} = \mathbf{g}_{SG} + \mathbf{g}_{LG} - \frac{4\mathbf{g}_{SG}^d \mathbf{g}_{LG}^d}{\mathbf{g}_{SG}^d + \mathbf{g}_{LG}^d} - \frac{4\mathbf{g}_{SG}^p \mathbf{g}_{LG}^p}{\mathbf{g}_{SG}^p + \mathbf{g}_{LG}^p} \quad (2.9.5)$$

Combining the Harmonic mean equation with Young's equation (2.9.1), the following equations are obtained:

$$(1 + \cos q_1) \mathbf{g}_{SL1} = 4 \left( \frac{\mathbf{g}_{SG}^d \mathbf{g}_{L1G}^d}{\mathbf{g}_{SG}^d + \mathbf{g}_{L1G}^d} + \frac{\mathbf{g}_{SG}^p \mathbf{g}_{L1G}^p}{\mathbf{g}_{SG}^p + \mathbf{g}_{L1G}^p} \right) \quad (2.9.6)$$

$$(1 + \cos q_2) \mathbf{g}_{SL2} = 4 \left( \frac{\mathbf{g}_{SG}^d \mathbf{g}_{L2G}^d}{\mathbf{g}_{SG}^d + \mathbf{g}_{L2G}^d} + \frac{\mathbf{g}_{SG}^p \mathbf{g}_{L2G}^p}{\mathbf{g}_{SG}^p + \mathbf{g}_{L2G}^p} \right) \quad (2.9.7)$$

where  $q_1$  and  $q_2$  are the contact angles of the liquids  $L_1$ , and  $L_2$ , and  $\mathbf{g}_{LV}^1$ ,  $\mathbf{g}_{LV}^2$ ,  $\mathbf{g}_{LV1}^d$ ,  $\mathbf{g}_{LV2}^d$ ,  $\mathbf{g}_{LV1}^p$ , and  $\mathbf{g}_{LV2}^p$  are the surface tension components of the liquid vapor, liquid dispersive, and liquid polar interactions of liquid one and two, respectively. Solving equations 2.9.6 and 2.9.7 simultaneously, the polar and dispersive forces of the surface tension of the solid can be determined and the surface tension of the solid can be obtained by:

$$\mathbf{g}_{SG} = \mathbf{g}_{SG}^d + \mathbf{g}_{SG}^p \quad (2.9.8)$$

The critical surface tension ( $\sigma_c$ ) developed by Zisman is a useful parameter to characterize how well a solid surface can be wetted, and is used to approximate the surface energy of the solid.<sup>43,48</sup> The critical surface tension of a solid can be found by measuring the contact angle of several weakly polar liquids on the solid.<sup>45-48</sup> An empirical linear relationship between the surface tension of the wetting liquid and the contact angle was found. The critical surface tension of the solid is determined by extrapolating the value to  $\cos\theta = 1$ .<sup>45-48</sup>

Table 2.9.1 Surface tension contributions for common liquids at 20°C used in determining surface energy from contact angle measurements<sup>47</sup>

Liquid	$\gamma_{LG}^p$ (dyne/cm)	$\gamma_{LG}^d$ (dyne/cm)	$\gamma_{LG}$ (dyne/cm)
Deionized Water	50.7	22.1	72.8
Methylene Iodide	6.7	44.1	50.8

#### 2.9.4 MEASURING ADHESIVE BOND STRENGTH OF TISSUE ADHESIVES

The measurement of the mechanical strength of an adhesive joint can be achieved using several joint geometries and testing methods including tensile testing of butt joints, peel tests, lap shear tests, cantilever beam tests, blister tests, etc.<sup>47</sup> In tissue adhesive testing, butt joints and lap shear tests have been used for bonding tissue, Figure 2.9.2. There has been no evidence in the literature of adhesive testing using a substrate other than harvested tissue. Initial adhesive testing on a surface such as glass with known and relatively constant surface tension could be used to compare adhesive bond strengths, without having to take into account the non-homogeneous surface of tissue. The surface tension of tissue is quite variable, since the material properties and amount of extracellular fluid vary by tissue function and species. In a clinical study, the critical surface tension measurements on human skin *in vivo* varied from  $19.3 \pm 1.8$  dyne/cm to  $35.5 \pm 2.8$  dyne/cm following treatment with various creams and ether.<sup>49</sup> The surface tension of pig intestinal mucosa was found to vary between 40 and 50 mN/m (dyne/cm) when tested in the presence of saline, gastric fluid and intestinal fluid.<sup>50</sup> The surface tension of glass is reported to be 56.8 dyne/cm and is comparatively high, compared to skin.<sup>51</sup> The adhesive bond strengths of several gelatin based tissue adhesives, fibrin glue and cyanoacrylate adhesives bonded to various tissue substrates is summarized in Table 2.9.2.



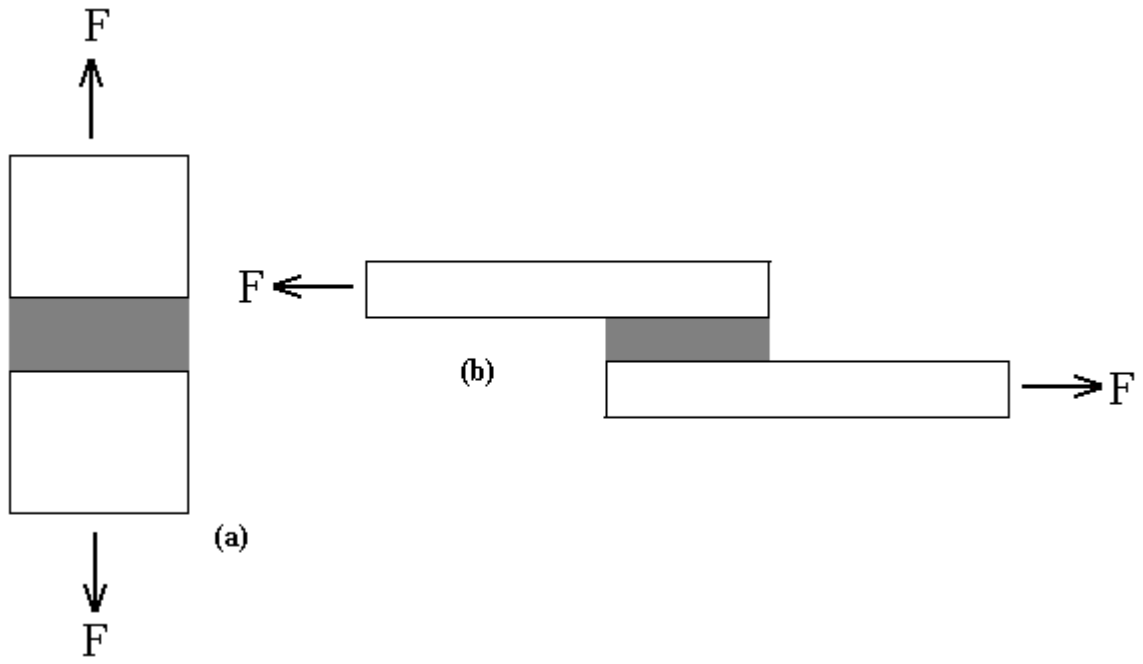


Figure 2.9.2 Butt joint test (a), lap shear joint test (b)<sup>47</sup>

Table 2.9.2 Summary of adhesive bond strengths found in the literature

Adhesive	Substrate	Test Joint Method	Test time after initial bond	Bond strength (kPa)	Note		
Gelatin/ Formaldehyde <sup>4</sup>	Cemented beef tissue plugs	Butt joint	5 min	19±3.2			
			15 min	39±4.9			
			1 hr	45±5.8			
			18 hr	23±5.9		Ringer's solution	
GRF <sup>4</sup>			5 min	26±5.4			
			15 min	49±5.1			
			1 hr	61±4.9			
			18 hr	91±12		Ringer's solution	
Polyurethane <sup>4</sup>			15 min	21±2.9			
			1 hr	34±3.1			
			18 hr	54±4.9		Ringer's solution	
Cyanoacrylate <sup>4</sup>			5 min	7.8±2.2			
			15 min	12±2.0			
			1 hr	20±3.1			
			18 hr	20±2.9		Ringer's solution	
Gelatin/ Glutaraldehyde <sup>29</sup>			Pig skin	Lap shear	N/A	25	
GRF <sup>52</sup>	Pig cartilage	Butt joint	N/A	150			
	Pig bone			200			
	Pig skin			70			
GR-DIAL <sup>52</sup>	Pig cartilage			21			
Cyanoacrylate <sup>52</sup>	Pig cartilage			1000			
	Pig bone			1400			
	Pig skin			1200			
	Pig cartilage			Lap shear	700		
Fibrin glue <sup>52</sup>	Pig cartilage			Butt joint	N/A	4.9	
	Pig bone					11	
	Pig skin	19					
	Pig skin	Lap shear	N/A	36	dermis-dermis		
				8.3	epidermis-epidermis		
GRFG <sup>53</sup>	Sheep thoracic aorta	Butt joint	N/A	13.8±10.0	Wet, 5 N applied		
				47.8±17.6	Wet, 20 N applied		
				35.0±16.4	Dry, 5 N applied		
				170.5±41.5	Dry, 20 N applied		

N/A: not available

## 2.9.5 BOND STRENGTH USING LAP SHEAR TEST

The lap shear test is the most widely used test for measuring bond strength<sup>47</sup> most likely due to the ease with which specimens may be prepared and tested, (Figure 2.9.3). In a lap joint, shear stresses are generated as a result of differential straining of the adhesive with respect to the adherend, in other words, the adhesive will deform by adapting to the displacement of the adherends.<sup>47</sup> Due to the geometry of the lap joint, complicated stresses may occur when the joint is loaded in tension. Eccentric loading may cause bending of the adherends, and tearing stresses normal to the interface.<sup>47</sup> Stress concentrations may exist at both ends of the overlap length  $l$ , and is dependent on the thickness and modulus of both the adherends and adhesive. Volkersen developed a model for determining the stress concentration factor based on differential straining of the adhesive, but neglected the stresses developed as a result of eccentric loading. Volkersen's equation<sup>47</sup> for stress concentration  $\alpha$ , is given by:

$$\mathbf{a} = \frac{\mathbf{t}_{\max}}{\mathbf{t}_{\text{ave}}} = \frac{\mathbf{d}}{\mathbf{e}} \left[ \frac{2\mathbf{e}^2 - 1 + \cosh(2\mathbf{e}\mathbf{d})}{\sinh(2\mathbf{e}\mathbf{d})} \right] \quad (2.9.9)$$

$$\mathbf{d}^2 = \frac{l^2 G}{E_2 t_2 t_a} \quad (2.9.10)$$

$$\mathbf{e}^2 = \frac{E_1 t_1 + E_2 t_2}{2E_1 t_1} \quad (2.9.11)$$

The modulus of the adherends are represented by  $E_1$  and  $E_2$ , the thickness of the adherends by  $t_1$  and  $t_2$ , the thickness and shear modulus of the adhesive by  $t_a$  and  $G$ , and the bond length is represented by  $l$ . Variables  $\epsilon$  and  $\delta$  are used for convenience in these equations. For equal adherends,  $E_1 t_1 = E_2 t_2$ , equation 2.9.9 reduces to:

$$\mathbf{a} = \mathbf{d} \coth \mathbf{d} \quad (2.9.12)$$

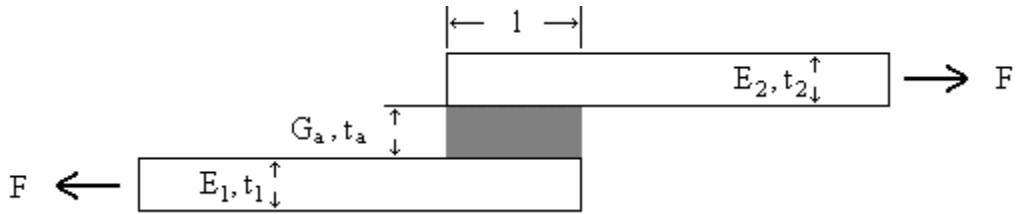


Figure 2.9.3 Dimensions of lap joint used in stress concentration equations

## 2.9.6 ADHESIVE FAILURE

There are three principle modes of failure used to identify failure of bonded joints.<sup>54</sup> Cohesive failure may occur in the adherends Figure 2.9.4 c, or in the adhesive, Figure 2.9.4 b. Cohesive failure of the adherend or adhesive is due to the weak properties of the bulk material. Failure of the adhesive bond may also occur at the interface, Figure 2.9.4 d. Weak intermolecular forces between the two surfaces cause interfacial failure.<sup>54</sup>

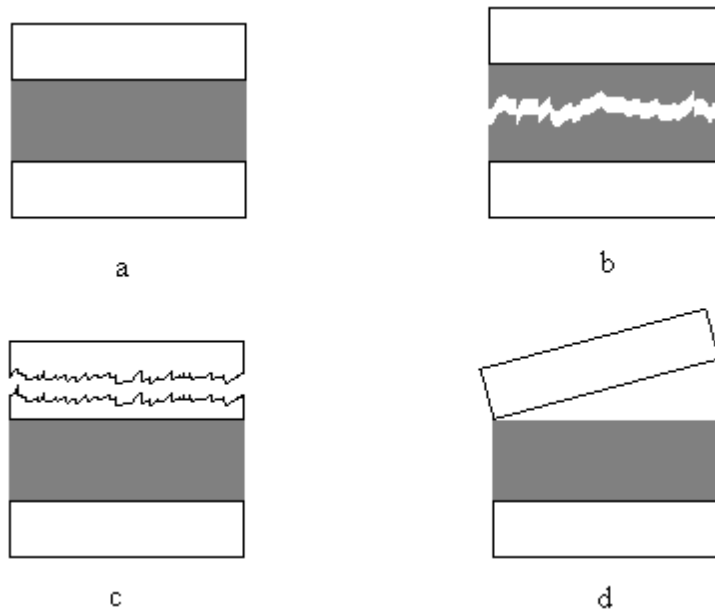


Figure 2.9.4 Adhesive bond (a), cohesive failure of adhesive (b), cohesive failure of adherend (c), and interfacial failure (d)